

Polariton bandstructure of disordered metallic photonic crystal slabs

D. Nau^{1,2}, A. Schönhardt^{*1}, D. N. Chigrin³, H. Kroha³, A. Christ⁴, and H. Giessen^{**2}

¹ Institut für Angewandte Physik, Universität Bonn, Wegelerstr. 8, D-53115 Bonn, Germany

² 4. Physikalisches Institut, Pfaffenwaldring 57, D-70569 Stuttgart, Germany

³ Physikalisches Institut, Universität Bonn, Nussallee 12, D-53115 Bonn, Germany

⁴ Max-Planck-Institut für Festkörperforschung, Heisenbergstr. 1, D-70569 Stuttgart, Germany

Received zzz, revised zzz, accepted zzz

Published online zzz

PACS 42.70.Qs, 64.60.Cn, 78.20.Bh, 78.40.Pg, 78.67.-n

We analyze the influence of disorder on the polaritonic bandstructure of metallic photonic crystal slabs. Different disorder types with varying next-neighbor correlations and disorder amounts are implemented. Angle-resolved transmission measurements allow to determine the relation of bandstructure and disorder. It is found that uncorrelated disorder retains the bandstructure and only reduces the splitting between the gaps. Correlated disorder, however, leads to the complete destruction of the bandstructure for moderate disorder amounts due to the excitation of different modes. We present a model that shows a good agreement with the measurements.

Copyright line will be provided by the publisher

1 Introduction

A lot of effort has been made in recent times to examine the optical properties of dielectric photonic crystals. The idea for these crystals arose several years ago, when they were discussed as materials to control radiative properties [1] or to localize light [2]. Especially the proposal to use photonic crystal structures for novel applications brought about fascinating concepts [3]. The idea behind these crystals is a perfect periodic variation of the dielectric constant, where the periodicity is on the order of the wavelength of light [4]. Such an arrangement can cause Bragg scattering of electromagnetic waves, resulting in stop bands in their electromagnetic transmission characteristics.

One problem arises when working with photonic crystals. Theory and device concepts always deal with perfect periodic structures, where the different dielectrics are arranged on perfect lattices. However, such crystals are artificially fabricated materials. Especially when working in the visible spectral range, the fabrication requirements often reach the limits of the utilized lithographic methods. Consequently, real photonic crystals can show strong deviations from the perfect structure [5]. Of course, such disorder directly influences the optical properties of real crystals [6]. Not only possible applications require a detailed knowledge about the influence of disorder in these artificial structures. From a fundamental point of view, the already interesting optical properties of photonic crystals show further interesting effects in the presence of disorder. Typical examples are disorder-induced modifications of photon states and of the transmission [2, 7, 8, 9].

The concept of *metallic* photonic crystals has gained a lot of interest recently [10]. In metal-based structures, one of the dielectric constituents is replaced by a metal. One possibility to fabricate such structures is the periodic arrangement of metallic nanostructures on top of a dielectric waveguide slab [11]. This

* Now at: Institut für Umweltphysik, Universität Bremen, 28359 Bremen, Germany

** Corresponding author: e-mail: giessen@physik.uni-stuttgart.de, Phone: +49 711 685 5111, Fax: +49 711 685 5097

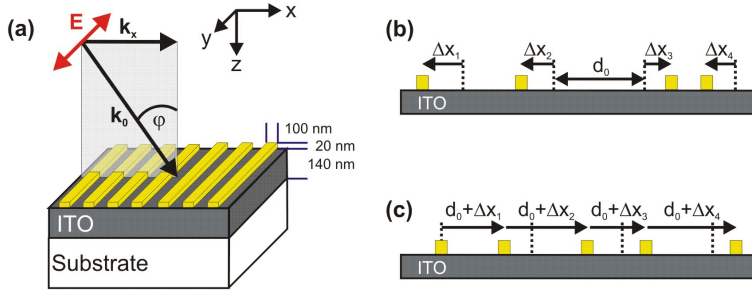


Fig. 1 (a): Metallic photonic crystal slab consisting of a gold grating on top of a dielectric waveguide layer. E indicates the direction of the electrical field polarization, φ denotes the angle of light incidence. (b) and (c): Scheme of uncorrelated and correlated disorder, respectively. Dotted lines indicate the center positions of the perfect grating with period d_0 .

metallic photonic crystal slab (MPCS) belongs to the class of crystals that provide simultaneously photonic and electronic resonances in the same spectral range. A strong coupling between the resonances due to the formation of a polariton-type quasiparticle comes along with a pronounced polaritonic bandstructure [12, 13].

It is the aim of this paper to enlighten the influence of disorder on the polaritonic bandstructure of MPCS. Therefore, a novel concept to study this relation in a quantitative way is utilized by artificially introducing disorder in a controlled manner into the structures. Measuring their optical properties allows to directly relate transmission spectra to disorder type and amount [14].

2 Sample description

Our samples consisted of one-dimensional gold gratings on top of a 140 nm thick dielectric waveguide layer (indium tin oxide, ITO), that was deposited on a glass substrate [Fig. 1(a)]. The width of the wires was 100 nm and their height 20 nm. By using electron-beam lithography to fabricate the samples, the positions and the shapes of the nanostructures can be controlled with very high accuracy when restricting to areas of less than $100 \times 100 \mu\text{m}^2$. Hence, we are able to introduce artificial disorder with a well defined type and strength into the crystal [14, 15]. The optical properties of the MPCS were measured with a white-light transmission setup with an aperture angle of about 0.2° [12]. The setup allowed for performing angle-resolved measurements by varying the polar angle of light incidence φ , see Fig. 1. When measuring the extinction $[-\ln(T), T$: transmission] of these structures, the influence of disorder type and amount on the polariton bandstructure of MPCS can be obtained.

It was found that the optical properties of such MPCS are determined by both the nanowires and the waveguide layer. An incident light field excites an electronic resonance in the metallic nanostructures (particle plasmon) [16]. Additionally, optical resonances in the waveguide layer are excited (see [13] and references therein). For symmetry reasons, only the symmetric quasiguided mode is excited at normal light incidence ($\varphi = 0$). The additional excitation of the antisymmetric quasiguided mode requires an oblique angle ($\varphi \neq 0$). Strong coupling effects of plasmon and quasiguided modes and the formation of a polariton-type quasiparticle were reported [12, 13]. For nanowires, the plasmon and hence the polariton can only be excited for light polarization perpendicular to the wires (TM polarization). In the extinction, the polariton is characterized at normal light incidence by two pronounced maxima that are separated by a spectral region with high transmission [11, 12]. These maxima are caused by the interaction of plasmon and symmetric quasiguided mode and they correspond to upper and lower polariton branch. For a polarization along the wires (TE polarization), only the highly asymmetric Fano-lineshape of the quasiguided mode is observable in the extinction [13]. The optical properties are strongly modified both in TE and TM polarization for

an oblique angle of incidence. The extinction shows an additional maxima which can be attributed to the excitation of the antisymmetric quasiguided mode [13].

3 Disorder Models

In this work, disorder means a variation of the positions of the nanowires (positional disorder). The width and the height of the nanowires are kept fixed. We consider two models with different next-neighbor correlations [14]. In the uncorrelated disorder model, the nanowires' positions are varied with respect to their positions in the perfect grid [Fig. 1(b)]. Starting at position x_0 , the position of nanowire i is given by

$$x_i = x_0 + i \cdot d_0 + \Delta x_i, \quad (1)$$

where d_0 is the period of the perfect grating and Δx_i is the variation of the i -th position. This model is related to phonons in a solid, where atoms and ions perform movements around their equilibrium positions due to thermal fluctuations [17]. In the correlated disorder model, the positions x_i and x_{i-1} of next-neighbors are correlated [Fig. 1(c)]. Therefore, x_i includes all variations of the preceding nanowires,

$$x_i = x_{i-1} + d_0 + \Delta x_i = x_0 + i \cdot d_0 + \sum_{j=1}^i \Delta x_j. \quad (2)$$

Similar methods are used to model amorphous materials [18]. A detailed discussion and characterization of the disorder models is reported in [14]. For normal light incidence, uncorrelated disorder reduces the excitation efficiency of the quasiguided mode which causes a reduced amplitude of the corresponding polariton branch [19]. Correlated disorder additionally excites several quasiguided modes at slightly different energies resulting in an inhomogeneous broadening of the extinction resonances. Furthermore, the coupling strength of the polariton was found to be disorder-dependent.

The variations Δx_i follow a uniform (rect) or a normal (Gaussian) distribution $D(\Delta x)$ with a full-width at half-maximum w . Giving w as a fraction of d_0 quantifies the disorder amount as $a[\%] = w/d_0 \cdot 100$ in the samples. In this work, we will determine the polaritonic bandstructures of samples with uniformly distributed uncorrelated disorder and with Gaussian distributed correlated disorder. It should be emphasized that the distribution $D(\Delta x)$ (uniform or normal) does not affect the qualitative effects at normal light incidence [14]; they are rather determined by the disorder type (correlated or uncorrelated). We therefore conclude that the qualitative effects that are presented in the following are also caused by the disorder type and not by $D(\Delta x)$.

4 Bandstructure

Figure 2 shows exemplary such angle-resolved extinction spectra in TE and TM polarization for the two different disorder types at 30% disorder amount. The polariton bandstructure can be deduced from the peaks of such measurements [12]. Therefore, the energies of the polariton resonances are plotted as a function of φ or of the momentum k_x with $k_x = k_0 \sin \varphi$ [see Fig. 1(a)]. The results for the sample with uniform uncorrelated disorder are shown in Fig. 3 (left panel) for increasing disorder. Clearly, the bandstructure of the polariton can be observed in the case of no disorder. It consists of pronounced bands that are separated by stop gaps. The bands correspond to lower, middle, and upper polariton branch, and the stop gaps are caused by the strong coupling in the MPCS. This bandstructure visualizes the interplay of particle plasmon, symmetric quasiguided mode, and antisymmetric quasiguided mode. Note, that the middle polariton branch (which corresponds to the antisymmetric quasiguided mode) does not appear at $k_x = 0$ for symmetry reasons. Increasing uniform uncorrelated disorder reduces the gaps between the bands. The splitting between the middle and upper polariton branches vanishes for a disorder amount of about 60%, and the splitting between upper and lower branch reduces continuously. The bandstructure itself is

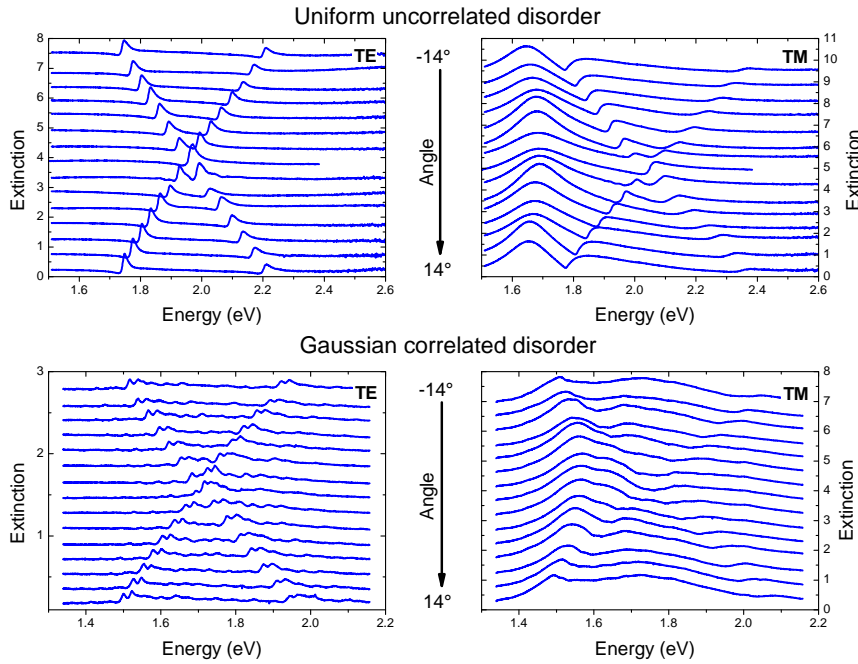


Fig. 2 Measured extinction spectra of samples with uniform uncorrelated disorder (upper panels) and Gaussian correlated disorder (lower panels), both for a disorder amount of 30%. The left (right) plots show spectra for TE (TM) polarization with increasing angle of light incidence φ .

retained and not destroyed by this type of disorder. Even for large disorder amounts of up to 70% the bands of the different polariton branches are distinguishable. For still larger amounts (80% and more) the quasiguided modes are not excited any more [14]. Thus, only the plasmonic polariton branch appears (not shown here).

The dispersion of the sample with Gaussian correlated disorder is plotted in the right panel of Fig. 3. For no disorder, again the polariton dispersion can be observed. Due to different detunings of plasmon and quasiguided mode in the samples, the bands appear at slightly different energies when compared to the sample with uniform uncorrelated disorder. Increasing disorder starts to wash out the bandstructure, and an amount of 30% and higher completely destroys the polariton branches. No bandstructure is retained, and further structures appear, causing the original polariton branches to be inhomogeneously broadened.

These results can be understood immediately when taking into account the results for disordered MPCS at normal light incidence [19]. Uncorrelated disorder reduces the amplitude of the polariton branch that corresponds to the quasiguided mode. Correlated disorder, however, additionally excites multiple quasiguided modes at different energies. We can attribute these modes to be responsible for the smearing of the bands for correlated disorder. Each mode couples to the plasmon and hence forms a polariton with slightly different energy and slightly shifted dispersion. The resulting dispersion of the sample leads to the complete vanishing of pronounced polariton branches. This is not the case for uncorrelated disorder with no additional quasiguided modes. It was also reported in [19] that disorder reduces the polariton splitting due to a modified coupling strength of the polariton. As the polariton splitting gives the energy separation of upper and lower branch in the bandstructure, this fact allows to analyze the decreasing stopbands for uncorrelated disorder. This effect also appears for correlated disorder, however, it is not visible there due to the smearing of the bands.

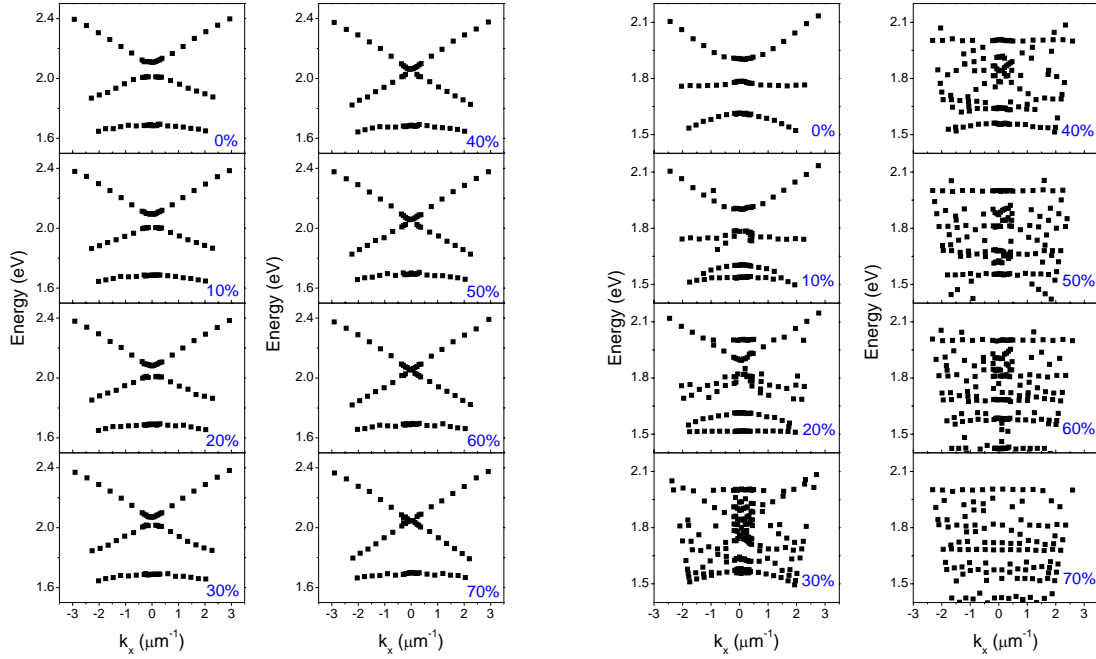


Fig. 3 Polaritonic bandstructure of a sample with increasing uniform uncorrelated disorder (left panel) and with increasing normal correlated disorder (right panel) in TM polarization. The dots denote peaks in the extinction spectra.

5 Simulation

The polariton dispersion of the *ordered* MPCS can be tailored by determining the eigenvalues of an effective Hamiltonian H_{eff} (see [12] for details). It includes the energy E_0 of the TM_0 quasiguided modes at $k_x = 0$, the energy E_{Pl} of the individual wire plasmons, the stop-band half-width V_1 in the 1-dim photonic crystal slab, and the coupling energy V_2 of quasiguided mode and wire plasmon. Absorption and losses are taken into account by introducing finite half-widths to the resonances of plasmon and quasiguided mode. With Γ as half-width of the plasmon, its energy E_{Pl} is replaced by $E_{Pl} - i\Gamma$. The same holds for the quasiguided modes, whose half-width γ modifies their energies to $E_0 \pm \tilde{c}k_x - i\gamma$. The radiative losses of the quasiguided modes are modelled with a complex photonic band gap. With γ_1 being the radiative damping, V_1 is replaced by $V_1 - i\gamma_1$. We obtain the following matrix to calculate H_{eff} [12]

$$\begin{pmatrix} E_0 + V_1 - i(\gamma + \gamma_1) & \tilde{c}k_x & \sqrt{2}V_2 \\ \tilde{c}k_x & E_0 - V_1 - i(\gamma - \gamma_1) & 0 \\ \sqrt{2}V_2 & 0 & E_{Pl} - i\Gamma \end{pmatrix}. \quad (3)$$

It was found that the coupling strength of plasmon and quasiguided mode is modified by disorder and defects [15, 20]. This can be understood intuitively as V_2 can be determined from the spatial overlap of the electrical fields of plasmon $\mathbf{E}_{Pl}(\mathbf{r})$ and quasiguided mode $\mathbf{E}_{WG}(\mathbf{r})$. In a system with positional disorder, this overlap can be drastically reduced. To quantitatively determine the decrease of V_2 , we calculate V_2 in

a simple model. Here, the modified coupling strength obeys

$$V_2^{dis} = \frac{1}{V_2} \int_{-\infty}^{\infty} \mathbf{E}_{WG} \cdot \mathbf{E}_{Pl} dx. \quad (4)$$

We normalize it to the coupling strength V_2 of the ordered MPCs. The modification of V_2 is then taken into account by replacing V_2 in Eq. (3) by $V_2^{mod} = V_2 \cdot V_2^{dis}$. The electrical field of the plasmon \mathbf{E}_{Pl} is mainly localized at the positions of the nanowires. Introducing disorder varies these positions. Hence, the coupling of plasmon and quasiguided mode is reduced in disordered systems due to a changing spatial overlap and a therefore modified V_2 [see Fig. 4(a)]. Approximating \mathbf{E}_{WG} by a cosine-type oscillation with period d_0

$$E_{WG}(x, \varphi) = \cos\left((2\pi x - \varphi)/d_0\right), \quad (5)$$

and assuming \mathbf{E}_{Pl} to be a non-zero constant inside the nanowires and vanishing outside

$$E_{Pl}(x) = \begin{cases} 1 & : x \in \text{nanowire} \\ 0 & : x \notin \text{nanowire} \end{cases}, \quad (6)$$

we estimate the change of V_2 by using the spatial arrangement of the nanowires. The results are shown in Fig. 4(b). V_2 decreases with increasing disorder, however, the models differ in the dependence of V_2 on the degree of disorder. Decreasing V_2 reduces the coupling of plasmon and quasiguided mode, causing a reduction of the polariton splitting in the dispersion.

With this Hamiltonian we are able to simulate the polariton dispersion of a MPCs with uncorrelated disorder. All parameters in Eq. (3) are adapted to yield the correct results for no disorder (see also the parameters in [12]). For larger disorder amount, only V_2^{mod} was changed according to Eq. (4). It should be noted that also the stop-band half-width V_1 of the 1-dim photonic crystal slab is influenced by disorder (see Section 6). However, we neglect this effect here.

The polariton bandstructure of a sample with uncorrelated disorder agrees well in experiment and simulation, as can be seen in Fig. 4(c). Increasing uncorrelated disorder retains the dispersion branches of the polariton, and the splittings between the bands are reproduced nicely by the simulations. Deviations in the simulated results from the measurements are presumably caused by not considering the influence of disorder on V_1 .

6 TE Polarization

We also determined the bandstructure in TE polarization, where only symmetric and antisymmetric quasiguided mode are excited at an oblique angle of incidence. Hence, the bandstructure reveals the dispersion of the quasiguided slab modes with two bands and not the one of the polariton. The results for the samples with uniform uncorrelated and with Gaussian correlated disorder are plotted in Figs. 5. Both bandstructures figure out nicely the observations from TM polarization. While uncorrelated disorder only reduces the splitting between both bands, additional modes occur for correlated disorder and broaden the bandstructure: No bandstructure is obtained for a disorder amount of about more than 20%. As pointed out in Section 4, the reduction of the bandsplitting due to uncorrelated disorder (see Fig. 5) indicates a modified V_1 in Eq. (3). Again, this can be understood intuitively as in such MPCs symmetric and antisymmetric quasiguided modes have their nodes and antinodes under the nanowires, respectively [13]. Hence, both modes experience a different effective dielectric environment, which leads to different energies according to their dispersion [21]. Introducing positional disorder modifies the positions of the nanowires with respect to both modes. As a result, the difference in the effective dielectric environment of symmetric and antisymmetric mode decreases, which leads to a reduced energy difference and hence a reduced splitting in the bandstructure.

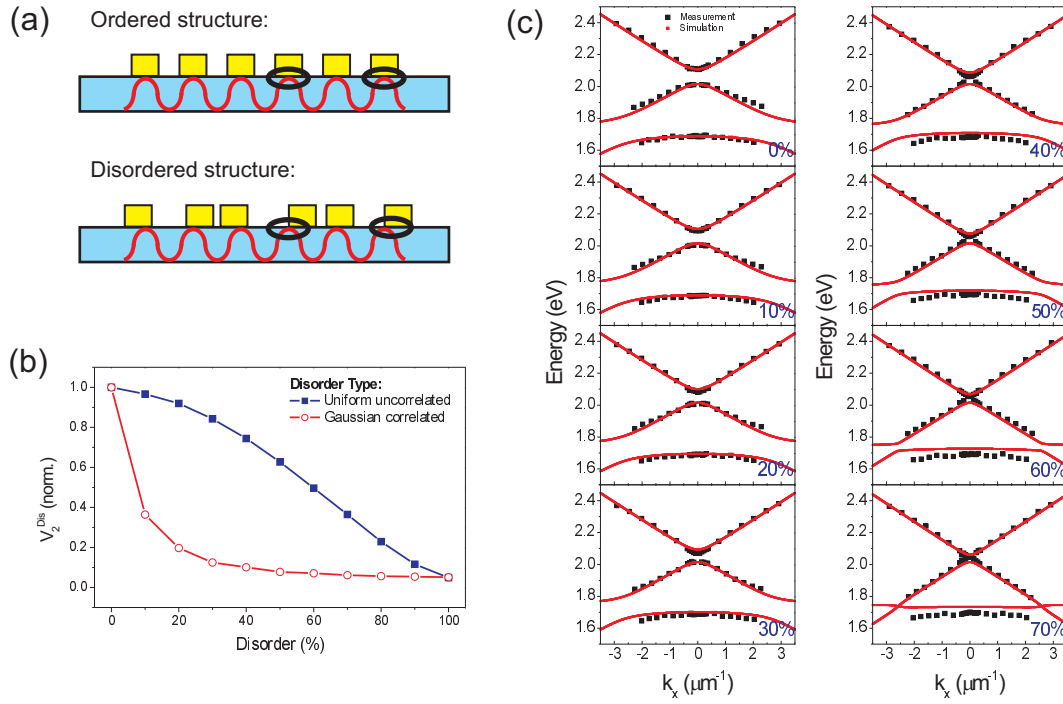


Fig. 4 (a) Spatial overlap of the electrical fields of plasmon and quasiguided mode in ordered and disordered MPCS. (b) Normalized modified coupling strength V_2^{mod} as a function of disorder and for different disorder types. (c) Dispersion of the sample with uniform uncorrelated disorder: experiment and simulation in TM polarization. The bandstructure is plotted for increasing amounts of disorder.

7 Conclusion

To conclude, we have studied the influence of disorder on the polariton bandstructure of metallic photonic crystal slabs. We found that uncorrelated disorder retains the bandstructure and only reduces the splitting between the bands. The latter can be explained by a reduced spatial overlap of the electrical fields of particle plasmon and quasiguided modes. Correlated disorder, however, leads to the excitation of several modes at slightly different energies. They cause a smearing of the bands and a total destruction of the bandstructure at moderate amount of disorder. Our results are interesting for improving possible future applications of MPCS on the one hand (see e.g. [22]), on the other hand they could give first hints to localization in our structures [2]. The limitations of this method are obvious for correlated long-range disorder: Due to the breakdown of the bandstructure, it is no longer possible to describe the system with a simple photonic band structure. Solid state physics describes a possible route to follow with its successful description of amorphous semiconductors. More elaborate concepts, such as mobility gaps, Urbach tails, and localized states within the gap shall be used.

Acknowledgements We thank S. G. Tikhodeev for fruitful discussions and the teams of R. Langen and K. D. Krause for technical support. Financial support by the German BMBF (FKZ 13N8340/1) and DFG (FOR 557 and SPP 1113) are gratefully acknowledged.

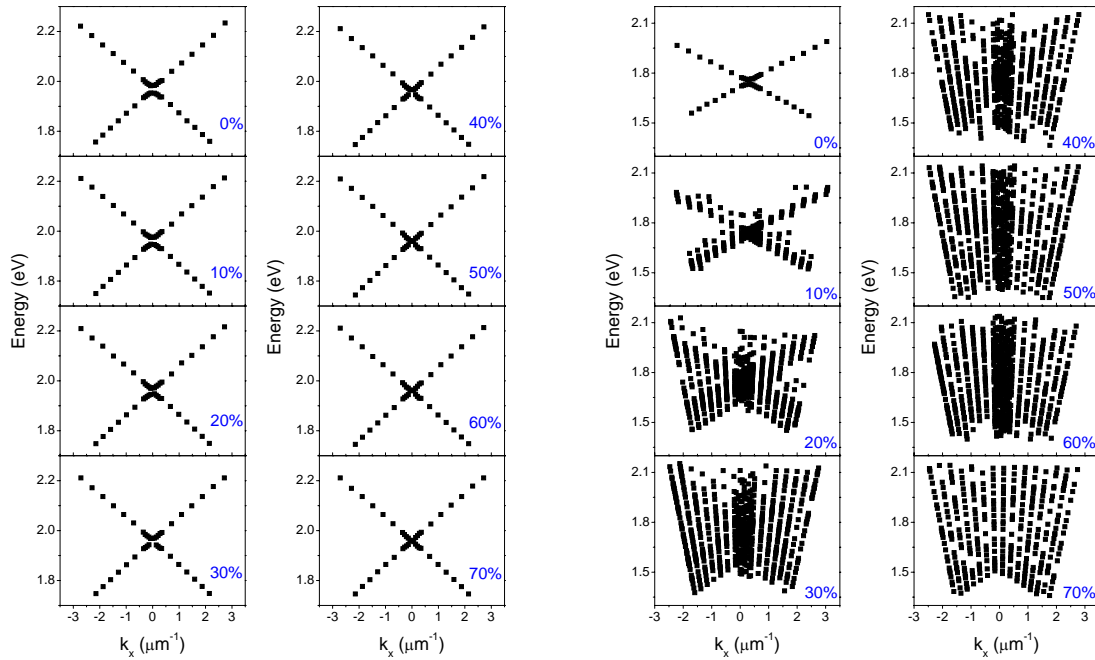


Fig. 5 Polariton bandstructure of a sample with increasing uniform uncorrelated disorder (left panel) and with increasing normal correlated disorder (right panel) in TE polarization.

References

- [1] E. Yablonovitch, *Phys. Rev. Lett.* **58**, 2059 (1987).
- [2] S. John, *Phys. Rev. Lett.* **58**, 2486 (1987).
- [3] T. F. Krauss, R. M. De La Rue, and S. Brand, *Nature* **383**, 699 (1996).
- [4] J. D. Joannopoulos, P. R. Villeneuve, and S. Fan, *Nature* **386**, 143 (1997).
- [5] Y. A. Vlasov, V. N. Astratov, A. V. Baryshev, A. A. Kaplyanski, O. Z. Karimov, and M. F. Limonov, *Phys. Rev. E* **61**, 5784 (2000).
- [6] A. F. Koenderink, A. Lagendijk, and W. L. Vos, *Phys. Rev. B* **72**, 153102 (2005).
- [7] V. D. Freilikher, B. A. Liansky, I. V. Yurkevich, A. A. Maradudin, and A. R. McGurn, *Phys. Rev. E* **51**, 6301 (1995).
- [8] J. Bertolotti, S. Gottardo, D. S. Wiersma, M. Ghulinyan, and L. Pavesi, *Phys. Rev. Lett.* **94**, 113903 (2005).
- [9] R. Sainidou, N. Stefanou, and A. Modinos, *Phys. Rev. Lett.* **94**, 205503 (2005).
- [10] E. R. Brown and O. B. McMahon, *Appl. Phys. Lett.* **67**, 2138 (1995).
- [11] S. Linden, J. Kuhl, and H. Giessen, *Phys. Rev. Lett.* **86**, 4688 (2001).
- [12] A. Christ, S. G. Tikhodeev, N. A. Gippius, J. Kuhl, and H. Giessen, *Phys. Rev. Lett.* **91**, 183901 (2003).
- [13] A. Christ, T. Zentgraf, J. Kuhl, S. G. Tikhodeev, N. A. Gippius, and H. Giessen, *Phys. Rev. B* **70**, 125113 (2004).
- [14] D. Nau, A. Schönhardt, C. Bauer, A. Christ, T. Zentgraf, J. Kuhl, and H. Giessen, *phys. stat. sol. (b)* **243**, 2331 (2006).
- [15] D. Nau, A. Christ, S. Linden, J. Kuhl, and H. Giessen, in: *CLEO/IQEC and PhAST Technical Digest on CDROM* (The Optical Society of America, Washington, DC, 2004), IThB6.
- [16] U. Kreibig and M. Vollmer, *Optical Properties of Metal Clusters* (Springer-Verlag, Berlin, 1995).
- [17] C. Kittel, *Introduction to Solid State Physics* (John Wiley & Sons, 1996).
- [18] K. Maschke, H. Overhof, and P. Thomas, *phys. stat. sol. (b)* **57**, 237 (1973).
- [19] D. Nau, A. Schönhardt, C. Bauer, A. Christ, T. Zentgraf, J. Kuhl, and H. Giessen, submitted.

-
- [20] T. Zentgraf, A. Christ, J. Kuhl, N. A. Gippius, S. G. Tikhodeev, D. Nau, and H. Giessen, *Phys. Rev. B* **73**, 115103 (2006).
 - [21] M. K. Barnoski, *Introduction to Integrated Optics* (Plenum Press, New York, 1974).
 - [22] D. Nau, R. P. Bertram, K. Buse, T. Zentgraf, J. Kuhl, S. G. Tikhodeev, N. A. Gippius, and H. Giessen, *Appl. Phys. B* **82**, 543 (2006).